

## CHAPTER THREE

### COMPUTED TOMOGRAPHY

#### 3.1 INTRODUCTION

The introduction of computed tomography (CT) marks the beginning of a new activity for the radiologic community. So remarkable is CT that it has been hailed as a revolutionary breakthrough in the history of medicine, as was the discovery of x-rays in 1895.

The basic concepts of CT have been extended to generate other imaging methods such as digital radiography and magnetic resonance imaging.

This chapter will introduce the relevant concepts of CT and will indicate how the fundamental principles of digital image processing have been incorporated into the acquisition of the CT image.

#### 3.2 CT - A DEFINITION

The term computed tomography (CT) implies that a computer is used in the acquisition of the image. It also means that some basic theory of tomography is used to produce the image. In essence, this theory involves the production of an image of specific layer of the body. For CT, the layer of interest is a cross-sectional layer that is totally free of superimposition of structures above and below the desired cross section. Such superimposition is one of the primary

shortcomings of radiography.

Conventional tomography (geometric tomography) can be used to eliminate the problem of superimposition of structures. However, there are other limitations imposed by conventional tomographic methods, such as image blurring which still persists and poor contrast resolution caused by the presence of scattered radiation due to the open beam geometry of the system.

In CT, these shortcomings are completely removed through the use of the following:

- (a) Special detectors.
- (b) Highly collimated x-ray beams.
- (c) Multiple x-ray transmission readings obtained through specific scanning (x-ray tube and detector motion) sequences.

In general, CT is a digital imaging technique based on similar steps involved in digital image processing theory. These steps involved:

- (a) Scanning the object, through special motions of the x-ray tube and detectors.
- (b) Sampling each portion of the density scanned by using special detectors to measure transmitted x-rays and converting them into electrical signals (analog data).
- (c) Quantization, where each measurement in (b) above is assigned a numerical value (digital data).



- (d) Processing the digital data with a digital computer.
- (e) Display and storage of the computer-processed image.

### 3.3 HISTORICAL BACKGROUND

Various aspects of the CT technique go back as far as 1917, when Radon<sup>(49)</sup> introduced the idea of using mathematics based on projection data to solve problems relating to the theory of gravity. Other workers then focussed their efforts on a basic theorem which dealt with reconstruction of an object by means of multiple projections of the object (image reconstruction from projections). This work led to the development of techniques which proved successful in astronomy, electron microscopy, optics and medicine (isotope and radiology).

In 1961, Oldendorf, Kuhl, Edwards and Cormack applied reconstruction techniques to solve medical problems. From 1967 to 1972, Hounsfield, working in England, developed and introduced the first clinically useful CT scanner.

#### 3.3.1 Hounsfield and Cormack - A Short Biography<sup>(50)</sup>

In 1972, Godfrey Newbold Hounsfield receive the equivalent of the Nobel Prize in Engineering for his work on CT. Hounsfield was born in England in 1919. He studied electronics at the Royal Air Force in Cranwell.

Later, he attended Faraday House where he graduated in electrical and mechanical engineering.

In 1951, he joined the staff at EMI (Electric and Musical Industries) and in 1967 he began working on pattern-recognition techniques which later gave birth to CT scanning.

In 1979, Hounsfield shared the Nobel Prize in Medicine and Physiology with Allan MacLeod Cormack, a physics professor at Tufts University in Medford, Massachusetts. Cormack was born in South Africa in 1924 and studied nuclear physics at Cambridge University. He is recognized for his contribution to CT, since he developed solutions to some of the mathematical problems involved in CT.

#### 3.4 PRINCIPLES OF X-RAY COMPUTED TOMOGRAPHY

If a narrow (small cross-sectional area) beam of monoenergetic x-ray photons passes through some homogeneous material, the beam intensity is observed to decrease in accordance with the equation

$$I = I_0 e^{-\mu x} \quad (3.1)$$

where  $I_0$  is the input intensity (number of photons per second per unit cross-sectional area) and  $I$  is the observed intensity after the beam passes a distance  $x$  through the material. The linear attenuation coefficient  $\mu$  depends on both the density of the material and the nuclear composition characterized by the atomic number  $Z$ ,



$$\mu = \mu(\rho, z).$$

In the following discussion, this dependence on  $\rho$  and  $z$  will not be shown explicitly.

If the x-ray beam passes through two different materials, distance  $x_1$  through medium 1 characterized by  $\mu_1$  and distance  $x_2$  through medium 2 characterized by  $\mu_2$ , the fractional decrease in intensity is given by

$$I/I_0 = \exp(\mu_1 x_1 - \mu_2 x_2).$$

For several media the relation is

$$I/I_0 = \exp[-\sum_j \mu_j x_j].$$

If  $\mu = \mu(x)$  is a continuous (or piecewise continuous) function of  $x$ , the sum goes over to an integral along the beam path  $L$ ,

$$I/I_0 = \exp[-\int_L \mu(x) dx] \quad (3.2)$$

Now, consider a transverse section through some three-dimensional object. If the transverse section plane is perpendicular to the  $z$  axis (of an orthogonal coordinate system), then the (variable) linear attenuation coefficient in the plane may be written as a function of two variables  $x$  and  $y$ , which coordinatize the  $xy$  plane,

$$\mu = \mu(x, y).$$

If the narrow beam traverses the  $xy$  plane as indicated in Figure 3.1, the fractional decrease in intensity is given by

$$I/I_0 = \exp[-\int_L \mu(x,y) ds] \quad (3.3)$$

where the line integral is along the beam path  $L$ . The natural logarithm of (3.3) yields a single projection,

$$P = -\ln(I/I_0) = \int_L \mu(x,y) ds. \quad (3.4)$$

By moving the source and detector as indicated in Figure 3.2, it is possible to obtain a set of projections or profile for the angle  $\theta$ ,

$$P(r,\theta) = \int_L \mu(x,y) ds. \quad (3.5)$$

In the complete scanning process, values of  $P(r,\theta)$  are determined for each family of parallel lines  $L(r,\theta)$  at various angles  $\theta$  by measuring the transmitted and incident intensities and employing (3.4). In theory, if  $P(r,\theta)$  is known for every line intersecting the section, the problem may be solved if (3.5) can be inverted. In practice, values of  $P(r,\theta)$  can only be determined for a finite number of lines, and the region of interest is divided into a number of small squares of dimension  $w$ , called picture elements or pixels, on which the absorption coefficient has a constant value.

The number and size of these pixels is determined by the nature of the scanning process.



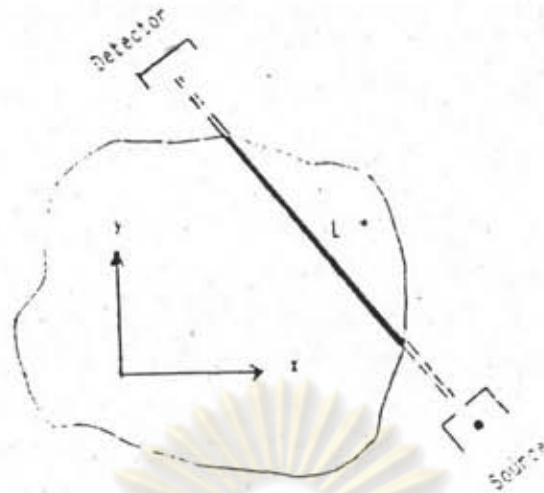


Figure 3.1 The beam pass through the region characterized by  $\mu(x,y)$  along the line  $L$

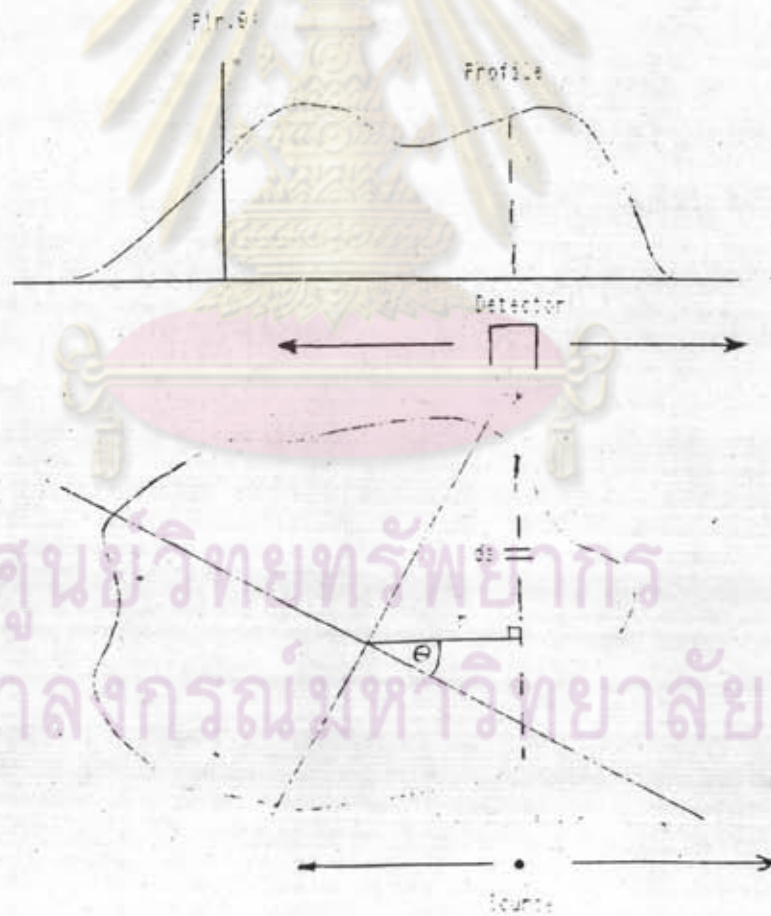


Figure 3.2 The source and detector move together ( $r$  varies) so that the beam covers the entire region leading to the profile  $F(r,\theta)$  for fixed angle  $\theta$ .

### 3.5 THEORY OF THE IMAGE RECONSTRUCTION IN COMPUTED TOMOGRAPHY

A theoretical solution, namely the determination of  $u(x,y)$  from (3.5), given  $P(r,0)$ , was first found by Radon(1917) in association with a gravitational problem. No numerical reconstruction was investigated, however, until Bracewell (1956). encountered the identical problem in radioastronomy, when attempting to identify regions in the sun which emitted microwave radiation. The identical mathematical problem was later encountered by workers studying complex biomolecules using electron microscopes, and independent solution techniques were developed by DeRosier and Klug(1968),<sup>(51)</sup> and Gordon, Bender and Herman(1970). Meanwhile, Cormack<sup>(52)</sup> (1963),<sup>(53)</sup> (1964), again independently of other workers, developed a reconstruction technique which he applied experimentally, and suggested the use of the process in transverse tomography. It was not until the early development of the commercial scanners, described above, however, that a coordinated effort was made in extending these techniques to transverse axial tomography.

At present a diversity of methods for reconstruction are available. One reference<sup>(54)</sup> (Budinger and Gullberg(1974)) lists 13 different methods which may be used in both transmission and emission tomography. However, it is possible to classify the various approaches broadly into four categories,<sup>(55-73)</sup>



namely

- (a) summation methods (e.g. simple back projection), (27,74-77)
- (b) series expansion methods (e.g. iterative estimate-correct), (20,25,34,78-96)
- (c) transform methods (e.g. Fourier transform), (18,24,52,53,97-116)
- (d) direct analytic methods (e.g. convolution or filtered back projection). (19,21-23,117-124)

In this section we emphasis present on the theory underlying the filtered-backprojection algorithm for which the computational procedures were presented in next section. Basic to the filtered-backprojection algorithms is the Fourier slice theorem.

### 3.5.1 The Fourier Slice Theorem

The Fourier slice theorem relates the one-dimensional Fourier transform of a projection of a function  $g(x,y)$  to its two-dimensional Fourier transform. Let  $G(u,v)$  be the Fourier transform of the image  $(x,y)$ , which implies that

$$G(u,v) = \int_{-\infty}^{\infty} \int_{-\infty}^{\infty} g(x,y) \exp[-j2\pi(ux+vy)] dx dy, \quad (3.6)$$

and

$$g(x,y) = \int_{-\infty}^{\infty} \int_{-\infty}^{\infty} G(u,v) \exp[j2\pi(ux+vy)] du dv \quad (3.7)$$

Also let  $S_{\theta}(w)$  be the Fourier transform of the projection  $P_{\theta}(t)$ , that is

$$S_{\theta}(w) = \int_{-\infty}^{\infty} P_{\theta}(t) \exp(-j2\pi wt) dt \quad (3.8)$$

Let us first consider the values of  $G(u,v)$  on the line  $v = 0$  in the  $uv$  plane. From equation (3.6)

$$\begin{aligned}
 G(u,0) &= \int_{-\infty}^{\infty} \int_{-\infty}^{\infty} g(x,y) \exp(-j2\pi ux) dx dy \\
 &= \int_{-\infty}^{\infty} \left[ \int_{-\infty}^{\infty} g(x,y) dy \right] \exp(-j2\pi ux) dx \\
 &= \int_{-\infty}^{\infty} P(t) \exp(-j2\pi ut) dt \\
 &= S(w) \tag{3.9}
 \end{aligned}$$

because  $\int g(x,y) dy$  gives the projection of the image for  $\theta = 0$ . Note that for this projection  $x$  and  $t$  are the same.

The preceding result indicates that the values of the Fourier transform  $G(u,v)$  on the line defined by  $v = 0$  can be obtained by Fourier transforming the vertical (along  $y$ ) projection of the image. This result can be generalized to show that if  $G(w,0)$  denotes the values of  $G(u,v)$  along a line at angle  $\theta$  with the  $u$  axis, as shown in Figure 3.3, and if  $S(w)$  is the Fourier transform of the projection  $P(t)$ , then

$$G(w, \theta) = S(w) \tag{3.10}$$

This can be proved as follows. Let  $g(t,s)$  be the function  $g(x,y)$  in the rotated coordinates system  $(t,s)$  in Figure 3.3. The coordinates  $(t,s)$  are related to the  $(x,y)$  coordinates by

$$\begin{bmatrix} t \\ s \end{bmatrix} = \begin{bmatrix} \cos\theta & \sin\theta \\ -\sin\theta & \cos\theta \end{bmatrix} \begin{bmatrix} x \\ y \end{bmatrix} \tag{3.11}$$

Clearly,



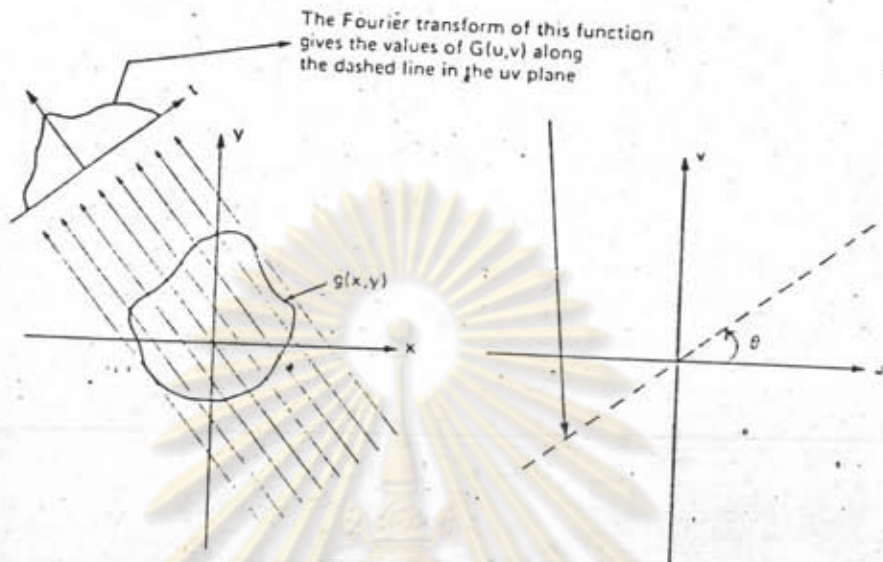


Figure 3.3 . Illustration of the Fourier slice theorem.

$$P_{\theta}(t) = \int_{-\infty}^{\infty} g(t,s) ds. \quad (3.12)$$

Therefore,

$$\begin{aligned} S_{\theta}(w) &= \int_{-\infty}^{\infty} P_{\theta}(t) \exp(-j2\pi wt) dt \\ &= \int_{-\infty}^{\infty} \int_{-\infty}^{\infty} g(t,s) ds \exp(-j2\pi wt) dt. \end{aligned} \quad (3.13)$$

Transforming the right-hand side of the above equation into xy coordinates, we obtain

$$\begin{aligned} S_{\theta}(w) &= \int_{-\infty}^{\infty} \int_{-\infty}^{\infty} g(x,y) \exp[-j2\pi w(x\cos\theta + y\sin\theta)] dx dy \\ &= G(u,v) \quad \text{for} \quad \begin{cases} u = w\cos\theta \\ v = w\sin\theta \end{cases} \\ &= G(w,\theta), \end{aligned} \quad (3.14)$$

which prove equation (3.10). This result is also known as the projection slice theorem.

### 3.5.2 Derivation of Filtered-Backprojection Equations for Parallel Data

If, as before,  $(w, \theta)$  are the polar coordinates in the  $uv$  plane, the integral in equation (3.7) can be expressed as

$$\begin{aligned} g(x, y) &= \int_0^{2\pi} \int_0^{\infty} G(w, \theta) \exp[j2\pi w(x\cos\theta + y\sin\theta)] w dw d\theta \\ &= \int_0^{\pi} \int_0^{\infty} G(w, \theta) \exp[j2\pi w(x\cos\theta + y\sin\theta)] w dw d\theta \\ &\quad + \int_0^{\pi} \int_0^{\infty} G(w, \theta + 180^\circ) \exp[j2\pi w(x\cos(\theta + 180^\circ) \\ &\quad + y\sin(\theta + 180^\circ))] w dw d\theta. \end{aligned}$$

Using the property  $G(w, \theta + 180^\circ) = G(-w, \theta)$ , we can write the preceding expression for  $g(x, y)$  as

$$\begin{aligned} g(x, y) &= \int_0^{\pi} \left[ \int_{-\infty}^{\infty} G(w, \theta) |w| \exp(j2\pi wt) dw \right] d\theta \\ &= \int_0^{\pi} \left[ \int_{-\infty}^{\infty} S(w) |w| \exp(j2\pi wt) dw \right] d\theta \quad (3.15) \end{aligned}$$

Where, as noted before,  $t = x\cos\theta + y\sin\theta$  and where we have used equation (3.14). The integral in equation (3.15) may be expressed as

$$g(x, y) = \int_0^{\pi} Q_{\theta}(x\cos\theta + y\sin\theta) d\theta \quad (3.16)$$

where

$$Q_{\theta}(t) = \int_{-\infty}^{\infty} S(w) |w| \exp(j2\pi wt) dw. \quad (3.17)$$

These two equations form the basics of the algorithm discussed in next chapter.